Extended local binary patterns for texture classification

Article *in* Image and Vision Computing · February 2012

DOI: 10.1016/j.imavis.2012.01.001

5 authors, including:

Li Liu
University of Oulu
48 PUBLICATIONS **2,490** CITATIONS
SEE PROFILE

Gangyao Kuang
National University of Defense Technology
237 PUBLICATIONS **2,442** CITATIONS
SEE PROFILE

Paul Fieguth
University of Waterloo
344 PUBLICATIONS **5,805** CITATIONS
SEE PROFILE

Generalized Local Binary Patterns for Texture Classification

Li Liu[1], ***Paul Fieguth***[2] and ***Gangyao Kuang***[1]

[1]School of Electronic Science and Engineering, National University of Defense Technology, China

[2]Department of System Design Engineering, University of Waterloo, Canada

Email: dreamliu2010@gmail.com; pfieguth@engmail.uwaterloo.ca and kuangyeats@vip.sina.com

1 Abstract

Goal: Simple, fast, yet powerful local descriptor for gray-scale and rotation invariant texture classification.

- Features: Local pixel intensities and differences
  → easy to compute, complementary information
- Feature space quantization: Proposing CI-LBP, NI-LBP and RD-LBP via LBP-type of quantization
  → off-the-shelf texton codebook, low computational complexity, training free
- Model: Joint histogramming
  → simple, powerful
- Classifier: Nearest neighbor classifier
  → simple

2 Introduction

The welcome BoW model benefits from two complementary components:

- *local* discriminative and robust texture descriptors → a crucial factor in superior texture classification.
- *global* statistical histogram characterization

Motivations:

- To inherit the advantages of the BoW model
- To enjoy the impressive computational efficiency of LBP
- To avoid the limitations of LBP
- To gain the benefits of combining complementary types of features

3 A Brief Review of LBP

Images are probed locally by sampling greyscale values at a central point $x_{0,0}$ and p points $x_{r,0}, ..., x_{r,p-1}$ spaced equidistantly around a circle of radius r centered at $x_{0,0}$, as shown in Fig.1. Formally,

$$LBP_{p,r} = \sum_{n=0}^{p-1} s(x_{r,n} - x_{0,0})2^n, \quad s(x) = \begin{cases} 1, x \geq 0 \\ 0, x < 0 \end{cases} \tag{1}$$

An $N \times M$ image $\mathbf{I}$ can be represented by a histogram vector $\underline{\boldsymbol{h}}$ of length $K = 2^p$.

The conventional LBP has disadvantages

- the overwhelming dimensionality of $\underline{\boldsymbol{h}}$ with large p
- very sensitive to noise

Therefore, a better descriptor – the so-called "uniform" pattern $LBP^{riu2}_{p,r}$, has been proposed

$$LBP^{riu2}_{p,r} = \begin{cases} \sum_{n=0}^{p-1} s(x_{r,n} - x_{0,0}), & \text{if } U(LBP_{p,r}) \leq 2 \\ p+1, & \text{otherwise} \end{cases} \tag{2}$$

where $U(LBP_{p,r}) = \sum_{n=0}^{p-1} |s(x_{r,n} - x_{0,0}) - s(x_{r,mod(n+1,p)} - x_{0,0})|$.

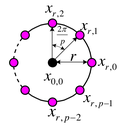

4 Our Approach

We have proposed four descriptors (shown in Fig. 2) with the same form as the conventional LBP codes, thus they can be readily combined to form joint histograms to represent textured images.

1. NI-LBP:

$$NI - LBP_{p,r} = \sum_{n=0}^{p-1} s(x_{r,n} - \mu)2^n, \quad \mu = \frac{1}{p}\sum_{n=0}^{p-1} x_{r,n} \tag{3}$$

Similar to $LBP^{riu2}_{p,r}$, the rotation invariant version of $NI - LBP$, denoted by $NI - LBP^{riu2}_{p,r}$, can also be defined to achieve rotation invariant classification.

2. CI-LBP

$$CI - LBP = s(x_{0,0} - \mu_I) \tag{4}$$

relative to μ_I, the mean of image $\mathbf{I}$.

3. RD-LBP

$$RD - LBP_{p,r,\delta} = \sum_{n=0}^{p-1} s(\Delta^{\text{Rad}}_{\delta,n})2^n \tag{5}$$

4. AD-LBP

$$AD - LBP_{p,r,\delta} = \sum_{n=0}^{p-1} s(\Delta^{\text{Ang}}_{\delta,n})2^n \tag{6}$$

The proportions of the uniform patterns of AD-LBP were too small (Fig. 3) and inadequate to provide a reliable and meaningful description of texture images. Consequently we prefer not to include the AD-LBP in our experiments.

The samples are then classified according to their normalized histogram feature vectors $\underline{\boldsymbol{h}}_i$ and $\underline{\boldsymbol{h}}_j$, using χ^2 distance metric $\chi^2(\underline{\boldsymbol{h}}_i, \underline{\boldsymbol{h}}_j) = \frac{1}{2}\sum_k \frac{[\underline{\boldsymbol{h}}_i(k) - \underline{\boldsymbol{h}}_j(k)]^2}{\underline{\boldsymbol{h}}_i(k) + \underline{\boldsymbol{h}}_j(k)}$.

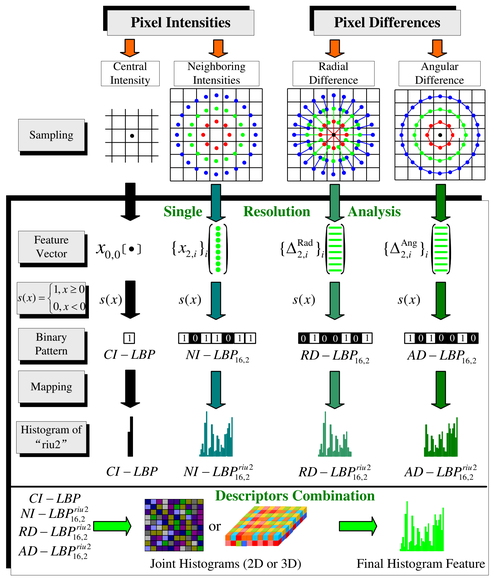

Fig. 2 Overview of the proposed approach

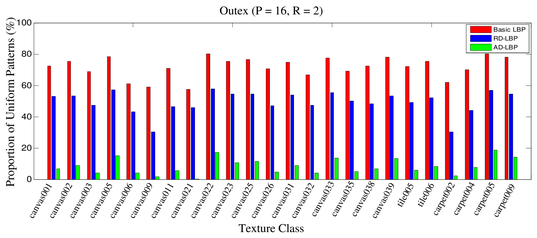

Fig. 3 Comparing the proportions (in %) of uniform patterns

5 Experimental Results

Table 1 Classification accuracies (%) on Contrib_TC_00001

Method	(p, r)	Bins	Rotation Angle for Train 0°	20°	30°	45°	60°	70°	90°	120°	135°	150°	Average
LBP	(16,2)	18	96.2	99.0	98.6	98.9	98.5	99.1	97.6	98.6	98.7	97.5	98.3
VAR	(16,2)	128	89.9	84.5	86.2	90.5	87.3	85.6	91.0	89.8	90.8	88.5	88.4
LBP/VAR	(8,1)+(16,2)+(24,3)	864	100	99.7	99.5	99.8	99.6	99.7	99.8	99.6	99.8	99.9	99.7
NI	(8,1)	10	65.4	85.5	81.3	76.6	77.0	78.4	68.8	81.4	75.8	76.5	76.7
	(16,2)	18	87.6	95.2	92.3	93.6	89.4	96.0	88.9	91.3	93.4	90.1	91.8
	(24,3)	26	96.2	93.4	97.6	96.6	98.3	96.7	97.1	96.7	92.6	98.2	96.4
RD	(8,1)	10	68.8	86.4	84.4	76.0	84.9	84.4	70.2	84.1	76.1	84.7	80.0
	(16,2)	18	89.2	92.9	96.7	97.8	96.1	92.6	88.4	94.7	96.7	97.3	94.3
	(24,3)	26	87.6	90.6	98.2	90.8	96.5	93.8	89.5	98.6	89.5	94.2	92.9
RD/CI	(8,1)	20	87.1	94.7	94.3	88.6	95.9	95.1	85.8	94.8	90.3	95.0	92.2
	(16,2)	36	92.7	94.6	96.8	97.3	98.4	95.6	91.8	99.4	96.7	98.6	96.2
	(24,3)	52	96.9	95.8	95.6	92.8	96.5	94.3	96.9	99.1	95.3	95.9	95.9
NI/CI	(8,1)	20	74.8	90.4	86.4	80.3	82.5	85.2	74.4	86.2	80.6	82.2	82.3
	(16,2)	36	95.6	99.2	98.8	98.0	98.2	99.4	93.8	98.3	96.9	97.4	97.6
	(24,3)	52	99.1	98.7	99.4	99.4	100	100	99.7	97.5	97.3	99.1	99.1
NI/RD	(8,1)	100	70.2	88.9	87.0	80.0	85.2	85.5	71.9	87.1	81.6	84.9	82.2
	(16,2)	324	**100**	**100**	**100**	**100**	**100**	**100**	**100**	**100**	**100**	**100**	**100**
	(24,3)	676	98.2	100	100	100	100	100	99.6	99.9	99.9	100	99.8
NI/RD/CI	(8,1)	200	78.1	94.5	92.2	91.1	93.0	92.0	76.2	92.4	91.8	92.6	89.4
	(16,2)	648	**100**	**100**	**100**	**100**	**100**	**100**	**100**	**100**	**100**	**100**	**100**
	(24,3)	1352	98.8	100	100	100	100	100	99.8	100	99.8	100	99.8

Table 2 Classification accuracies (%) for all the three Outex test suites

Test Suite	Outex_TC_00012 "tl84", (p, r)	(8, 1)	(16, 2)	(24, 3)	Outex_TC_00012 "horizon" (8, 1)	(16, 2)	(24, 3)	Outex_TC_00010 "inca" (8, 1)	(16, 2)	(24, 3)	Mean Accuracy (8, 1)	(16, 2)	(24, 3)
LBP		67.5	81.2	84.0	62.7	74.1	80.5	85.1	88.5	94.6	71.8	81.3	86.4
VAR		64.3	67.1	62.6	64.7	72.5	68.9	91.2	90.7	86.2	73.4	76.8	72.6
LBP/VAR		78.8	86.1	86.6	76.7	84.8	87.2	95.4	97.2	97.8	83.6	89.4	90.5
NI		59.1	71.9	76.3	56.2	65.5	72.2	76.4	87.0	88.7	63.9	74.8	79.1
RD		67.0	77.4	76.8	63.1	72.3	72.1	81.0	86.6	89.7	70.4	78.8	79.5
NI/CI		76.5	88.6	88.9	77.4	89.4	84.6	89.9	96.4	95.7	81.3	91.5	89.7
RD/CI		87.9	91.9	86.1	88.3	91.5	82.3	95.2	95.9	93.7	90.7	93.1	87.4
NI/RD		79.0	96.2	95.2	80.8	95.2	92.2	88.9	98.7	98.8	82.9	96.7	95.4
NI/RD/CI		90.9	**98.0**	97.3	92.7	98.0	96.2	96.5	**99.3**	99.2	93.4	**98.4**	97.6

Table 3 Classification accuracy (%) of descriptor $NI/RD/CI$ for the three Outex test suites (training is done at just one rotation angle)

Test Suite	(p, r)	Rotation Angle for Train "inca" 0°	5°	10°	15°	30°	45°	60°	75°	90°	Average
Outex_TC_00012 ("tl84")	(8,1)	90.9	91.6	92.1	93.0	91.3	90.8	88.9	89.0	84.3	90.2
	(16,2)	98.0	98.3	99.1	98.6	98.4	98.6	98.6	97.7	96.8	98.3
	(24,3)	97.3	98.3	98.5	98.7	97.2	96.4	93.4	94.2	94.1	96.5
	(8,1)+(16,2)	97.4	98.0	98.4	98.5	98.3	98.3	97.8	97.1	95.6	97.7
	(8,1)+(24,3)	97.7	98.3	98.7	98.7	98.5	97.9	96.4	96.6	96.4	97.7
	(16,2)+(24,3)	98.3	99.0	99.3	99.2	98.9	98.9	98.3	98.1	98.1	**98.7**
	(8,1)+(16,2)+(24,3)	98.5	98.9	99.1	99.1	99.0	98.9	98.4	98.2	98.1	**98.7**
Outex_TC_00012 ("horizon")	(8,1)	92.7	92.8	93.3	93.6	92.7	91.6	90.3	91.1	86.6	91.6
	(16,2)	98.0	98.0	98.3	98.4	97.7	97.9	98.2	98.3	98.1	**98.1**
	(24,3)	96.2	97.0	97.0	97.3	95.5	95.1	92.7	93.7	94.1	95.4
	(8,1)+(16,2)	98.2	97.8	98.3	97.9	97.1	97.8	98.2	97.8	97.0	97.8
	(8,1)+(24,3)	97.8	97.5	97.7	97.7	96.2	96.1	95.1	95.2	95.1	96.3
	(16,2)+(24,3)	97.8	98.3	98.2	98.3	97.3	97.5	96.9	97.0	97.7	97.7
	(8,1)+(16,2)+(24,3)	97.8	98.4	98.4	98.2	97.4	97.7	97.5	97.1	97.6	97.8
Outex_TC_00010 ("inca")	(8,1)	96.5	96.3	97.4	97.6	96.2	95.3	92.7	94.9	91.8	95.4
	(16,2)	99.3	99.4	99.5	99.7	99.6	99.6	99.5	99.0	99.0	99.4
	(24,3)	99.2	99.5	99.4	99.5	99.5	99.5	99.2	99.3	99.1	99.4
	(8,1)+(16,2)	99.4	99.4	99.6	99.6	99.5	99.4	99.4	99.0	98.6	99.3
	(8,1)+(24,3)	99.3	99.5	99.5	99.5	99.6	99.6	99.7	99.4	99.2	99.5
	(16,2)+(24,3)	99.6	99.7	99.8	99.7	99.7	99.9	99.8	99.7	99.5	**99.7**
	(8,1)+(16,2)+(24,3)	99.7	99.7	99.7	99.6	99.6	99.8	99.9	99.7	99.4	**99.7**

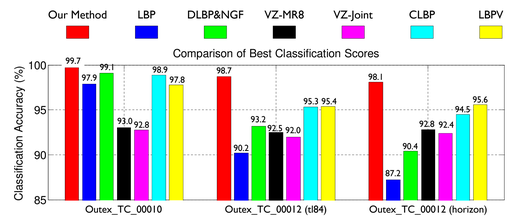

Fig. 4 Classification results (%) on Outex datesets: our method vs. state-of-the-art methods

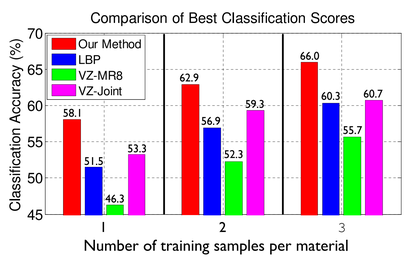

Fig. 5 Classification results (%) on KTHTIPS2b: our method vs. state-of-the-art methods